 

# Photophysical and Photochemical Processes of Poly(methylphenylsilane) Functionalized with Pendant *p*-Nitroazobenzene Groups

**Changli Zhao, Hiroaki Horiuchi, Tetsuo Okutsu, Seiji Tobita, Shoji Takigami, and Hiroshi Hiratsuka***

Department of Chemistry, Gunma University, Kiryu, Gunma 376-8515

(Received December 6, 2002)

The synthesis of poly(methylphenylsilane) functionalized with pendant *p*-nitroazobenzene groups (PMPS-azo) has been carried out, and their photophysical and photochemical processes have been studied. The fluorescence quantum yields of PMPS-azo decrease with an increase of the amounts of the pendant *p*-nitroazobenzene groups. The picosecond fluorescence decay kinetics of PMPS-azo was interpreted in terms of not only the energy transfer, but also the electron transfer from the Si–Si main chain to the pendant *p*-nitroazobenzene group. The evidence for intramolecular electron transfer was provided by the formation of the radical anion of the pendant *trans*-*p*-nitroazobenzene group upon steady-state photolysis of PMPS-azo at 77 K.

Polysilanes have attracted considerable interest due to their potential applications as nonlinear optical materials,[1–3] optical switches,[4] and photorefractive materials.[5–8] Because of the delocalization of the $\sigma$-electrons in the Si–Si main chain, polysilanes show unique photoelectric and photochemical properties.[9–14]

Recently, much attention has been focused on the introduction of functional groups into the side chain of polysilanes in order to provide a broader range of properties.[7,8,15–20] When chromophores are introduced as a pendant group to the polysilane backbones, they influence the electric properties, as well as the photochemical and photophysical behavior. The photoconductivity and electro-optical effects of poly(methylphenylsilane) with the pendant Disperse-Red 1 chromophore have been studied.[7,8] These polysilanes have been recognized as good candidates for photorefractive and third-order nonlinear optical materials. Amphiphilic polysilane bearing chiral pendant ammonia groups[15,16] and polysilane with phenol groups[17] have been investigated for highly oriented Langmuir–Blodgett films. Kminek and co-workers[18] have reported the synthesis and photochemical properties of poly(methylphenylsilane) modified by the attachment of $\pi$-conjugated chromophores. They found that these $\pi$-conjugated substituents in poly(methylphenylsilane) could significantly increase the photostability of the polysilane even at relatively low degrees of substitution. This stability was ascribed to the excitation energy transfer from the excited polysilane singlet states to the chromophoric groups. Nešpůrek and co-workers[19] have also prepared poly(methylphenylsilane) modified by the $\pi$-conjugated side groups and shown that the introduction of the pendant group generated photoluminescence in the visible region. Tachibana and co-workers[20] synthesized helical polysilanes bearing Rhodamine B and demonstrated that the energy transfer to the luminescence center by the transport of photogenerated free excitons on the Si–Si backbones was realized. It is of interest, therefore, to prepare polysilanes with pendant chromophores and to investigate their photophysical and photochemical processes as a basis for application.

We investigated the functionalized polysilanes with pendant *p*-nitroazobenzene groups. From the point of view of molecular design, the functionalized polysilanes would contain the necessary elements for photorefractive materials with a sensitizer (charge generator), photoconductor (charge transport agent), and a nonlinear optical dye for the modulation of the refractive index.[21,22] This is a novel photorefractive polymer with a Si–Si main chain suitable as photoconductor and a pendant *p*-nitroazobenzene group as the nonlinear optical chromophore. So far, only hole transport in polysilanes has been reported,[23] while electron transport has become important as a charge generator for photorefractive materials.[24] An azobenzene with an electron acceptor, such as a *p*-nitro group linked to the side chain of the polysilanes, would be expected to induce the efficient intramolecular electron transport in these polysilanes.

In this paper, we report on the photophysical and photochemical processes of poly(methylphenylsilane) functionalized by *p*-nitroazobenzene groups (PMPS-azo) with various degrees of substitution. We expected that the pendant *p*-nitroazobenzene groups would interact with the $\sigma$-electrons in the Si–Si main chain. The photophysical processes have been investigated by the fluorescence spectra and picosecond fluorescence lifetime measurements in solution. In order to obtain the evidence for electron transfer, steady-state photolysis was carried out in 2-methyltetrahydrofuran at 77 K by the irradiation with 266 nm light.

## Experimental

**Materials.** Tetrabutylammonium bromide (98.0%), chloromethyl methyl ether (80.0%), tin(Ⅳ) chloride (anhydrous, 97.0%), and chloroform (dehydration 99.0%, water <0.003%) were purchased from Wako Pure Chemical Industries Ltd. Tetrahydrofuran (THF, dehydrated, 99.5%, water <0.005%) was supplied from Kanto Chemical Co. Inc. THF (analytical grade, with-

out stabilizer), cyclohexane (analytical grade), and $CDCl_3$ (99.7%, without TMS), provided by Wako Pure Chemical Industries Ltd., were used as received for spectroscopic measurements. Poly(methylphenylsilane) (PMPS), obtained from Gelest Inc., was reprecipitated three times by pouring its THF solution into an excess of methanol before use. 2-Methyltetrahydrofuran (MTHF, anhydrous, 99%, inhibited with 250 ppm butylated hydroxytoluene), supplied by Sigma-Aldrich Fine Chemicals, was distilled to remove the inhibitor according to the literature.[25]

**Synthesis.** 4-Hydroxy-4′-nitroazobenzene and 4-methoxy-4′-nitroazobenzene were prepared and purified by column chromatography with silica gel using acetone-petroleum ether as eluant followed by recrystallization from acetone.[26,27]

The synthetic route of PMPS-azo is shown in Scheme 1.

**Chloromethylated PMPS (CPMPS).** PMPS was chloromethylated using chloromethyl methyl ether and the mild Lewis acid, tin(Ⅳ) chloride, as a catalyst. The chloromethylated PMPS, with various degrees of substitution, was obtained by controlling the reaction time and the ratio of chloromethyl methyl ether and tin(Ⅳ) chloride.[28–31]

**PMPS Functionalized with *p*-Nitroazobenzene groups (PMPS-azo).** PMPS-azo was prepared by condensation of CPMPS with potassium salt of 4-hydroxy-4′-nitroazobenzene. This reaction is similar to the chromophore-functionalization of polystyrenes.[32,33] The chloromethyl groups of the polysilane were completely substituted by the *p*-nitroazobenzene groups. For example, PMPS-azo0.15 was prepared as follows, where 0.15 represents the mole fraction of the pendant *p*-nitroazobenzene groups in PMPS-azo. In a three-necked flask equipped with a condenser, magnetic stirrer, and argon inlet, 4-hydroxy-4′-nitroazobenzene (0.50 g) and 0.11 g of KOH were dissolved in a 20 mL of dehydrated THF. The solution was refluxed for 48 h. After cooling to room temperature, the 30 mL of THF solution of CPMPS0.15 (where 0.15 represents the mole fraction of chloromethyl units in CPMPS) (0.80 g) and tetrabutylammonium bromide (0.02 g) was slowly dropped into the flask from a funnel under argon atmosphere. The solution was stirred for 48 h at room temperature, and then refluxed for 48 h at 65 °C. The solution was concentrated and 100 mL of methanol was added. The brown red deposit was collected, washed with water, and successively extracted in a Soxhlet's extractor with methanol for 4 days, until the liquid was colorless. Then the solid was dissolved in THF and precipitated with methanol repeatedly. The product was dried under vacuum (Yield 54%).

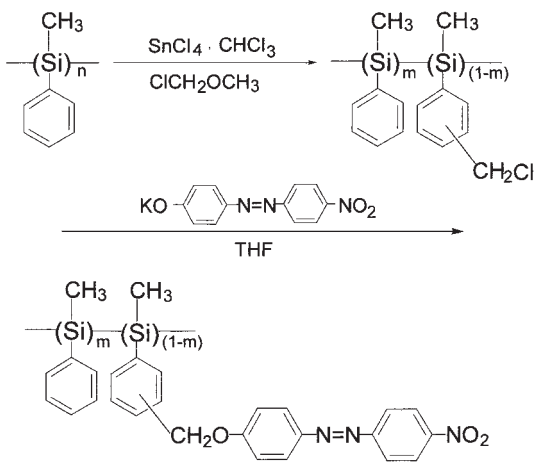


Scheme 1. Synthetic route of PMPS-azo.

**Measurements.** FT-IR spectra were recorded on a JASCO 8000 FT-IR spectrophotometer (KBr pieces); $^1$H NMR spectra were determined using a JEOL $\alpha$-500 FT-NMR spectrometer at 500 MHz. The chemical shifts were referenced to the residual solvent peak of $CDCl_3$ ($\delta = 7.24$ ppm). The number average molecular weights ($M_n$) and polydispersity ($M_w/M_n$) were determined by the gel permeation chromatography (Tosoh HLC-8120GPC) using a column (Tosoh TSK gel $\alpha$-M). Measurements were carried out using a UV detector at room temperature with a flow rate of 0.6 mL/min. The column was calibrated using polystyrene standards in THF.

Absorption spectra were recorded on a HITACHI U3300 spectrophotometer. Fluorescence emission and excitation spectra were determined by a HITACHI F4500 fluorescence spectrophotometer. The fluorescence quantum yields ($\Phi_f$) were measured by comparison with the fluorescence intensity of 2-naphthol ($\Phi_f = 0.32$ in cyclohexane[34]) as a reference.

The fluorescence decays were measured by a picosecond laser system of which instrumental response function is about 20–25 ps (FWHM). The apparatus was based on a mode-locked Ti:Sapphire laser (Spectra Physics, Tsunami; 800 nm, FWHM ~70 fs, at 82 MHz), and pumped by a CW green laser (Spectra Physics Millennia V, 532 nm, 4.5 W). The repetition rate was adjusted to 4 MHz by using a pulse-picker (Spectra Physics, Model 3980), and the third harmonic (266 nm, FWHM ~250 fs) was used as the excitation source. The monitoring system consisted of a microchannel-plate (MCP) and photomultiplier tube (Hamamatsu R3809U-51) cooled to −20 °C, and a single-photon counting module (Becker and Hickl SPC-530). The fluorescence photon signal detected by the MCP detector and the photon signal of the second harmonic (400 nm) of the Ti:Sapphire laser were used for the start and stop pulses of the time-to-amplitude converter (TAC). The absorbance of the sample solution was adjusted to be 0.10 at the excitation wavelength.

Steady-state photolysis was carried out using the 266 nm light output of an $Nd^{3+}$:YAG laser (Quanta-Ray GCR-130, Spectra Physics, 5 mJ/pulse). The sample solution in a cell of 1 mm was fully bubbled with argon and frozen by liquid nitrogen just before use.

## Results and Discussion

**Characterization of PMPS-azo.** The chemical structure and the composition of resultant PMPS-azo were determined by FT-IR and $^1$H NMR spectra.

Figure 1 shows FT-IR spectra of PMPS (a), CPMPS0.15 (b), and PMPS-azo0.15 (c). The band due to the C–Cl stretching vibration is observed at 610 $cm^{-1}$ only for CPMPS0.15. The IR spectrum of PMPS-azo0.15 shows new absorption bands at 1520 and 1345 $cm^{-1}$ (indicated by the arrow), which are not observed for CPMPS0.15. These bands are ascribed to the asymmetrical and symmetrical stretching vibrations of $NO_2$ group. For the Si–O–Si and Si–OH stretching vibrations, broad IR signals are expected to be observed around 1100 and 900 $cm^{-1}$, respectively.[35] No such broad band, however, was detected, indicating that the Si–O–Si and Si–OH groups do not exist in these polysilanes.

Figure 2 shows $^1$H NMR spectra of CPMPS0.15 (a) and PMPS-azo0.15 (b). It is recognized that the chloromethyl group ($\delta = 4.46$ ppm, 2H) disappears in PMPS-azo0.15, and the $CH_2O$ group ($\delta = 4.88$ ppm, 2H) and phenyl hydrogen

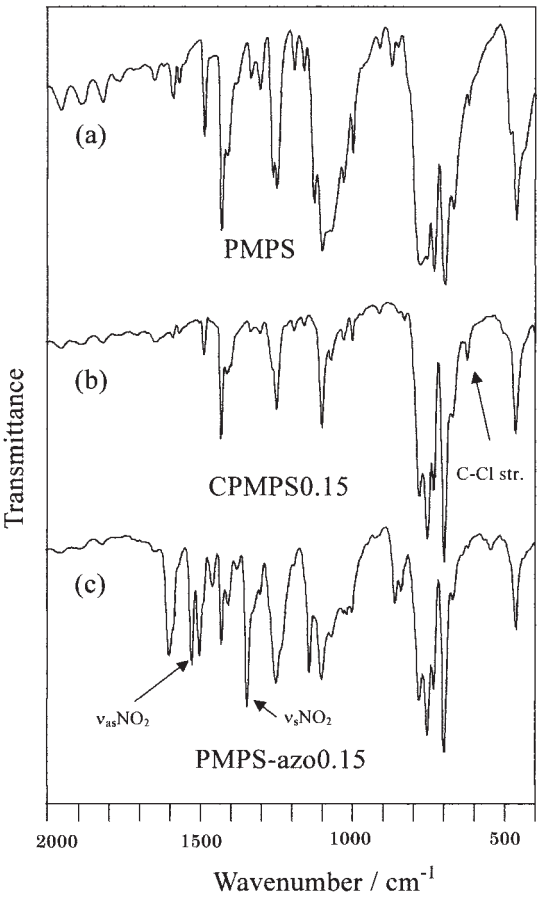


Fig. 1. FT-IR spectra of PMPS (a), CPMPS0.15 (b), and PMPS-azo0.15 (c).

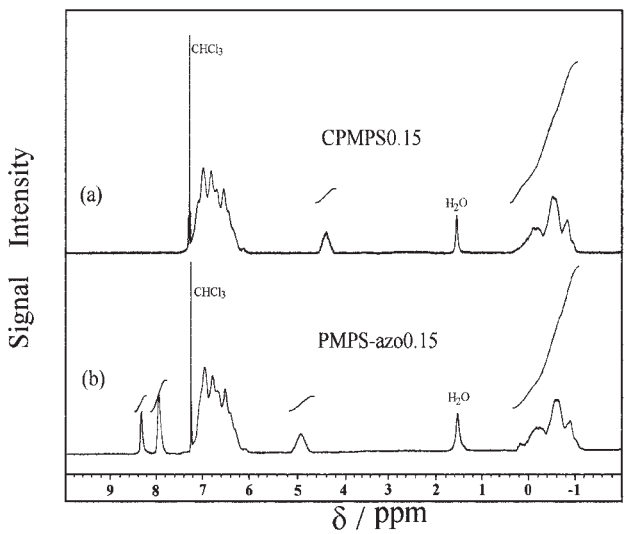


Fig. 2. $^1$H NMR spectra of CPMPS0.15 (a) and PMPS-azo0.15 (b).

of *p*-nitroazobenzene ($\delta = 8.35$ ppm, 2H adjacent to $NO_2$ group; $\delta = 7.84$ ppm, 4H adjacent to –N=N– group) are observed, indicating that the chloromethyl groups were completely substituted by the *p*-nitroazobenzene groups. Terunuma[16] and Jones[31] reported that the chloromethylation took place at the *para*-position on the phenyl rings due to steric hindrance.

Table 1. Properties of PMPS and PMPS-azo

| Sample | $f_A$[a)] | $M_n$ | $M_w/M_n$ | No. of units[b)] |
|---|---|---|---|---|
| PMPS | 0 | $11300 \pm 1500$ | 2.35 | $94 \pm 12$ |
| PMPS-azo0.01 | 0.01 | $10400 \pm 1100$ | 2.06 | $85 \pm 9$ |
| PMPS-azo0.07 | 0.07 | $16300 \pm 1300$ | 1.80 | $118 \pm 9$ |
| PMPS-azo0.15 | 0.15 | $11100 \pm 1400$ | 1.81 | $70 \pm 9$ |
| PMPS-azo0.32 | 0.32 | $15700 \pm 1100$ | 1.65 | $77 \pm 5$ |

a) $f_A$: the mole fraction of the pendant *p*-nitroazobenzene groups in PMPS-azo. b) No. of units was calculated from $M_n$.

According to their discussion, the resultant pendant *p*-nitroazobenzene group is believed to bond at the *para*-position of the phenyl rings of PMPS. The mole fraction ($f_A$) of pendant *p*-nitroazobenzene groups in PMPS-azo was determined by the integration of the signals of $CH_2O$ ($\delta = 4.88$) and $CH_3$ ($\delta = -1.2$ to 0.4) in the $^1$H NMR spectra. These results are summarized in Table 1.

The molecular weight of PMPS-azo was determined by GPC using polystyrene as a standard. Table 1 also shows the number average molecular weight ($M_n$) and polydispersity ($M_w/M_n$). The no. of units (the number average degree of polymerization) was calculated from $M_n$ to be 94 and 70–118 for PMPS and PMPS-azo, as shown in Table 1. The values for PMPS, PMPS-azo0.01 and PMPS-azo0.07 are close to each other, while those for PMPS-azo0.15 and PMPS-azo0.32 slightly decrease. This indicates the Si–Si main chain was not degraded by the introduction of lower mole fraction of pendant *p*-nitroazobenzene groups. With an increase in the mole fraction of pendant *p*-nitroazobenzene groups, the Si–Si main chain was slightly degraded.

**UV-Vis Absorption Spectra.** The UV-vis absorption spectra of PMPS and PMPS-azo with various mole fractions in THF at room temperature are shown in Fig. 3a. The absorption band peaked at ca. 340 nm is attributed to the $\sigma$–$\sigma^*$ transition of the Si–Si main chain of PMPS-azo in the *trans*-conformation.[36] The absorption band attributed to the pendant *trans*-*p*-nitroazobenzene group is observed around 375 nm. The molar extinction coefficient ($\varepsilon_{Si}$) of the Si–Si main chain was estimated by subtracting of the absorbance of the pendant *p*-nitroazobenzene group from the total absorbance at 340 nm, and $\varepsilon_{azo}$ of the pendant *trans*-*p*-nitroazobenzene group at 375 nm was estimated, as shown in Table 2. The molar extinction coefficient of *trans*-4-methoxy-4′-nitroazobenzene [MNAB] is also shown in Table 2 as a reference. The small difference in the molar extinction coefficients, both for the Si–Si main chain, and for the pendant *p*-nitroazobenzene group is ascribable to the weak electronic interaction between the Si–Si main chain and the pendant *p*-nitroazobenzene group in the ground state. From the integrated value of the molar extinction coefficient over the absorption band we derived the value of the radiative decay rate ($1/\tau_{Si}$) per Si unit.[14] The radiative decay rate of PMPS-azo, as shown in Table 2, is almost the same as that of PMPS. Therefore, the length of the segment of PMPS-azo (i.e., the number of Si atoms in each segment) is not changed by the introduction of the *p*-nitroazobenzene group. Also, the absorption spectra of these polysilanes in MTHF at 77 K are shown in Fig. 3b. There is a slight blue shift of the absorption maximum of the Si–Si main chain at

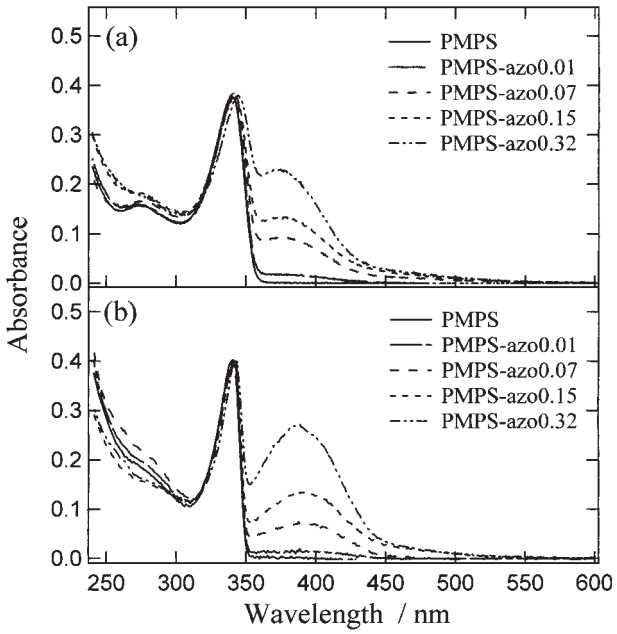


Fig. 3. The absorption spectra of PMPS and PMPS-azo in THF at room temperature (a) and in MTHF at 77 K (b).

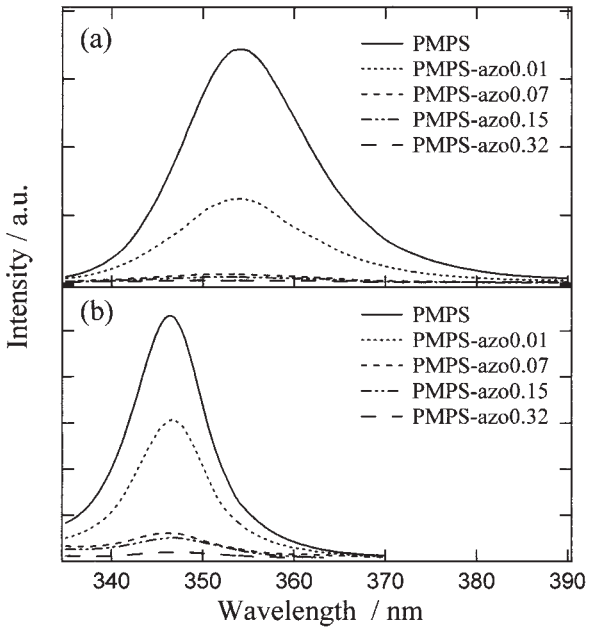


Fig. 4. The fluorescence emission spectra observed upon 328 nm excitation of PMPS and PMPS-azo in THF at room temperature (a) and in MTHF at 77 K (b). The absorbance at excitation wavelength of all samples was set to 0.1.

77 K compared with that at room temperature. However, the absorption band due to pendant *trans*-*p*-nitroazobenzene groups shows a red shift by 10 nm. Therefore, the overlap between the absorption bands of the Si–Si main chain and the pendant *p*-nitroazobenzene group is smaller at 77 K than it is at room temperature.

**Steady-State Fluorescence Quenching.** Figure 4a shows the fluorescence emission spectra observed upon 328 nm excitation of PMPS and PMPS-azo in THF at room temperature. The absorbance at the excitation wavelength of all samples was set to 0.1. The fluorescence bands peaked at 355 nm are due to the $\sigma$–$\sigma^*$ transition of the Si–Si main chain. The emission due to the pendant *p*-nitroazobenzene group was not observed as usual.[37] The fluorescence excitation spectrum monitored at 355 nm is similar to the corresponding absorption spectrum except for a small red shift. Figure 4b shows the fluorescence emission spectra observed upon 328 nm excitation of PMPS and PMPS-azo in MTHF at 77 K. The fluorescence emission maximum at 77 K was blue-shifted by 7 nm compared with that at room temperature. The spectral resemblance in the emission between the Si–Si main chain of PMPS-azo and PMPS indicates that a complex such as an exciplex between the Si–Si main chain and the pendant *p*-nitroazobenzene group was not formed even in the excited state.

The fluorescence quantum yields ($\Phi_f$) were determined by Eq. 1 using 2-naphthol as a reference ($\Phi_f = 0.32$ in cyclohexane[34]):

$$(\Phi_f)_{sam}/(\Phi_f)_{ref} = [(I_{EM})_{sam}/(I_{EM})_{ref}](A_{ref}/A_{sam}) \times [(I_{EX})_{ref}/(I_{EX})_{sam}](n_{sam}/n_{ref})^2 \quad (1)$$

where subscripts "sam" and "ref" denote the sample and reference, respectively. $I_{EM}$ is the integrated emission intensity. $A$, $I_{EX}$, and $n$ are absorbance at the excitation wavelength (328 nm), intensity of excitation light, and refractive index of sol-

Table 2. Photophysical Parameters for PMPS and PMPS-azo

| Sample | $\varepsilon_{Si}$[a] / mol$^{-1}$ cm$^{-1}$ L | $\varepsilon_{azo}$[b] / mol$^{-1}$ cm$^{-1}$ L | $1/\tau_{Si}$[c] / $10^9$ s$^{-1}$ | $\Phi_f$[d] | $\tau_{fl}$[e] / $10^{-9}$ s | $1/\tau_{rad}$[f] / $10^9$ s$^{-1}$ | $\tau_{Si}/\tau_{rad}$[g] |
|---|---|---|---|---|---|---|---|
| PMPS | 8100 | — | 0.11 | $0.15 \pm 0.01$ | 0.084 | 1.79 | 16 |
| PMPS-azo0.01 | 8150 | 31000 | 0.11 | $0.055 \pm 0.010$ | — | — | — |
| PMPS-azo0.07 | 8790 | 31000 | 0.13 | $0.008 \pm 0.002$ | — | — | — |
| PMPS-azo0.15 | 7900 | 24000 | 0.12 | $0.006 \pm 0.002$ | — | — | — |
| PMPS-azo0.32 | 8500 | 25000 | 0.13 | $\sim 0$[h] | — | — | — |
| MNAB[i] | — | 29000 | — | — | — | — | — |

a) $\varepsilon_{Si}$: the molar extinction coefficient of the Si–Si main chain (error within 2%). b) $\varepsilon_{azo}$: the molar extinction coefficient of the pendant *p*-nitroazobenzene group (error within 5%). c) $1/\tau_{Si}$: the radiative decay rate per Si unit. d) $\Phi_f$: the fluorescence quantum yield. e) $\tau_{fl}$: the fluorescence lifetime. f) $1/\tau_{rad}$: the radiative emission rate ($\Phi_f/\tau_{fl}$). g) $\tau_{Si}/\tau_{rad}$: the number of excitated Si atoms. h) The fluorescence is too weak to measure accurately. i) MNAB: *trans*-4-methoxy-4′-nitroazobenzene.

Table 3. Fluorescence Quenching Efficiency and Other Parameters for PMPS-azo

| Sample | $\chi$[a)] | $N_{Si}$[b)] | $n_{Si}$[c)] |
|---|---|---|---|
| PMPS-azo0.01 | 0.63 | 63 | 4 |
| PMPS-azo0.07 | 0.95 | 14 | <1 |
| PMPS-azo0.15 | 0.96 | 6 | <1 |

a) $\chi$: the fluorescence quenching efficiency. b) $N_{Si}$: the number of Si atoms quenched by each pendant *p*-nitroazobenzene group. c) $n_{Si}$: the number of segments of polysilane quenched by each pendant *p*-nitroazobenzene group.

vents averaged around the radiation wavelength, respectively. The results are shown in Table 2. The $\Phi_f$ value of 0.15 determined for PMPS is comparable with the reported values (0.08–0.3),[13] which varies with the molecular weight and excitation wavelength. In these polysilanes, $\Phi_f$ decreases with an increase of the mole fraction ($f_A$) of pendant *p*-nitroazobenzene groups; the fluorescence of the Si–Si main chain is quenched by the pendant *p*-nitroazobenzene group. At $f_A = 0.32$, $\Phi_f$ is almost zero.

The radiative emission rate ($1/\tau_{rad}$) of PMPS was calculated from the ratio of the fluorescence quantum yield ($\Phi_f$) and the fluorescence lifetime $\tau_{f1}$ (as will be seen in the following section). The ratio $\tau_{Si}/\tau_{rad}$ is a measure of the number of silicon atoms over which the excitation is delocalized.[14] The calculated result, as shown in Table 2, indicates the excited segment of PMPS consists of about 16 Si atoms, being in good agreement with the reported number of Si atoms (10–30) for each excited segment.[14,36] From the above discussion, therefore, the number of Si atoms in each excited segment of PMPS-azo is considered to be the same as that of PMPS (16 Si atoms). Since the average number of units of PMPS is about 94 (shown in Table 1), the average number of segments is estimated to be 6.

The quenching efficiency $\chi$ was calculated from the fluorescence quantum yield as follows,

$$\chi = 1 - [(\Phi_f)_{PMPS\text{-}azo}/(\Phi_f)_{PMPS}] \quad (2)$$

Table 3 shows values of $\chi$ for PMPS-azo in THF at room temperature. The number of Si atoms quenched by each pendant *p*-nitroazobenzene group, $N_{Si}$, was determined using the following equation:

$$N_{Si} = \chi/f_A \quad (3)$$

This type of equation was introduced by Holden et al.[38] to analyze the steady-state fluorescence quenching of the naphthalene chromophore by the ketone group in 2-vinylnaphthalene-phenyl vinyl ketone copolymers. The values of $N_{Si}$, as shown in Table 3, decrease with an increase of $f_A$. Therefore, the number of segments quenched by each pendant *p*-nitroazobenzene group ($n_{Si}$) was given by $N_{Si}/16 = 4$ for PMPS-azo0.01. The apparent value of $n_{Si} < 1$ was obtained for others, as shown in Table 3.

If the dynamic quenching mechanism is responsible for the fluorescence quenching of the Si–Si main chain by the pendant *p*-nitroazobenzene group, the following equation should be satisfied:

$$(I_f)_{PMPS}/(I_f)_{PMPS\text{-}azo} = 1 + \tau_{f1} k_q f_A \quad (4)$$

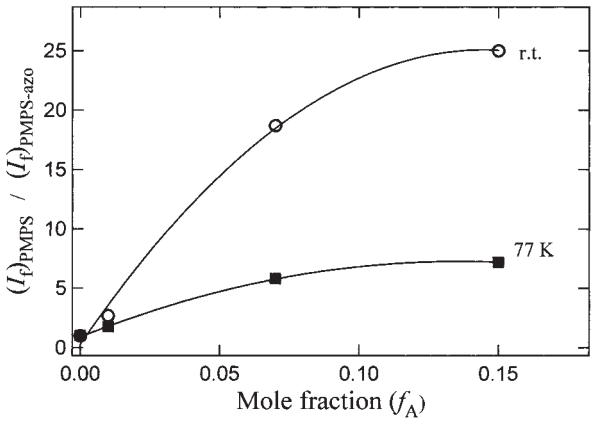


Fig. 5. The Stern-Volmer plots for the fluorescence quenching of the Si–Si main chain by the pendant *p*-nitroazobenzene group in PMPS-azo in THF at room temperature (open circle) and in MTHF at 77 K (full square).

where $\tau_{f1}$ and $k_q$ are the excited-state lifetime of PMPS and the quenching rate constant, respectively. Thus the Stern-Volmer plots [$(I_f)_{PMPS}/(I_f)_{PMPS\text{-}azo}$ vs $f_A$] are expected to give a straight line. However, the plots at room temperature shown in Fig. 5 (open circle) are curved, which indicates that static quenching occurs in the PMPS-azo system. The Stern–Volmer plots at 77 K also give a curve as shown in Fig. 5 (full square). This is evidence for static fluorescence quenching. By comparing these Stern-Volmer plots in Fig. 5, it is clear that the fluorescence of the Si–Si main chain is more efficiently quenched at room temperature than it is at 77 K.

This type of intramolecular quenching is attributable to the following processes: (1) energy transfer, (2) electron transfer, and (3) exciplex formation.[39] Among them, exciplex formation upon excitation of PMPS-azo, however, was not observed by nanosecond laser photolysis in THF at room temperature. Förster type energy transfer from the Si–Si main chain to the pendant *p*-nitroazobenzene group is considered to be possible in this system. The spectral overlap between the donor fluorescence and the acceptor absorption is necessary for the energy transfer. In our case, as shown in Fig. 6, the overlap between the emission (maximum at 355 nm) of the Si–Si main chain and the absorption (maximum at 375 nm) of the pendant *p*-nitroazobenzene group at room temperature is larger than it is at 77 K, where the maxima of the emission and absorption are 348 nm and 385 nm, respectively. This difference in spectral overlap may explain the difference in the quenching efficiency and deviations from the straight line shown in Fig. 5. Thus, the fluorescence quenching seems to be due to the Förster type energy transfer. It is noted that the shoulder at 365 nm observed in the fluorescence spectrum at room temperature in Fig. 6a is due to Raman scattering.

**Fluorescence Decay Kinetics.** Figure 7 illustrates the fluorescence decays of PMPS and PMPS-azo0.07 observed at 355 nm upon 266 nm laser pulse excitation in THF at room temperature. The decay curve $I_F(t)$ of PMPS was analyzed by a single exponential function with the fluorescence decay lifetime ($\tau_{f1}$) of 84 ps,

$$I_F(t) = B_1 \exp(-t/\tau_{f1}) \quad (5)$$

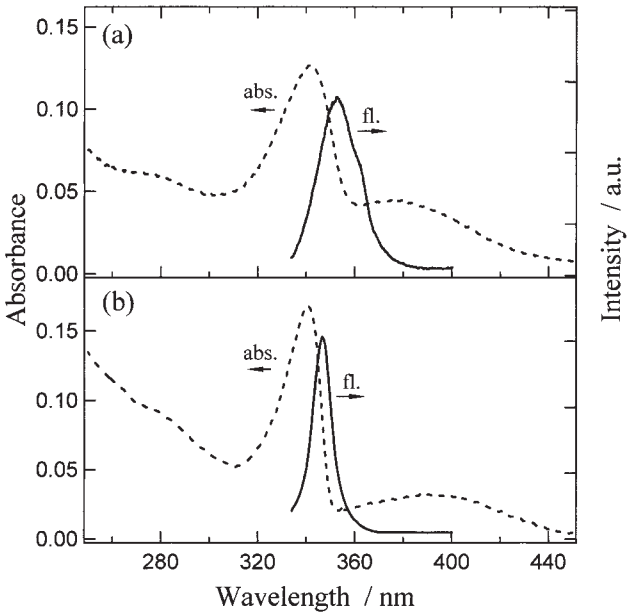


Fig. 6. The absorption (broken line) and fluorescence (full line) (exc. 328 nm) spectra of PMPS-azo0.07 in THF at room temperature (a) and in MTHF at 77 K (b).

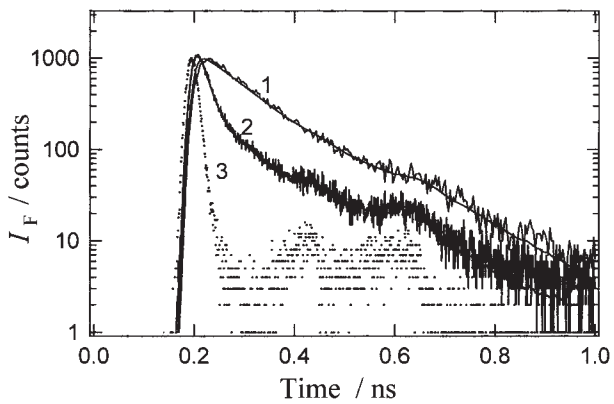


Fig. 7. Fluorescence decays of PMPS and PMPS-azo0.07 observed at 355 nm upon 266 nm laser pulse excitation in THF at room temperature. PMPS, curve 1; PMPS-azo0.07, 2; Laser pulse, 3.

where $B_1$ is a preexponential factor. The decay of PMPS-azo0.07, however, cannot be analyzed by a single exponential function but by the following double exponential function,

$$I_F(t) = B_1 \exp(-t/\tau_{f1}) + B_2 \exp(-t/\tau_{f2}) \quad (6)$$

where $B_1$ and $B_2$ are preexponential factors, and $\tau_{f1}$ and $\tau_{f2}$ are lifetimes for the long and short lifetime components, respectively. The analytical results are shown in Table 4. The value of $\tau_{f1}$ is kept constant (~83 ps), but the relative emission intensity due to the long lifetime component ($RI_1$) gradually decreases with an increase of $f_A$, while the value of $\tau_{f2}$ decreases with an increase of $f_A$ and the relative emission intensity due to the short lifetime component ($RI_2$) increases. Shortening in lifetime clearly indicates that the fluorescence of the Si–Si main chain of PMPS-azo is quenched by the pendant *p*-nitroazobenzene group.

Figure 8a shows the fluorescence response functions determined for PMPS and PMPS-azo. It is confirmed that the following function is not available for PMPS-azo from the point of view of fluorescence decay,

$$\mathrm{Ln}[I_F(t)] = -t/\tau_{f1} - k_q f_A t + \text{const.} \quad (7)$$

which is valid for Stern-Volmer kinetics.

We further studied whether the decay curves can be fitted by one-step Förster type kinetics or not. In Förster's formulation of the dipole-dipole energy transfer between molecules distributed randomly in a rigid environment, we have

$$\mathrm{Ln}[I_F(t)] = -t/\tau_{f1} - 1.127\pi^{3/2} C_A R_0^3 (t/\tau_{f1})^{1/2} + \text{const.} \quad (8)$$

where $C_A$ is the concentration of acceptor molecules, and $R_0$, called the critical energy transfer distance, is a measure of the strength of the dipole-dipole coupling.[40] The term $-F(t)$, gi-

Table 4. Analytical Results of Fluorescence Decays of PMPS and PMPS-azo

| Sample | $\tau_{f1}$/ps[a] | $B_1$[b] | $RI_1$/%[c] | $\tau_{f2}$/ps[a] | $B_2$[b] | $RI_2$/%[c] |
|---|---|---|---|---|---|---|
| PMPS | 84 | 0.179 | 100 | — | — | — |
| PMPS-azo0.01 | 80 | 0.108 | 79.4 | 22 | 0.101 | 20.6 |
| PMPS-azo0.07 | 83 | 0.067 | 66.0 | 13 | 0.220 | 34.0 |
| PMPS-azo0.15 | 85 | 0.057 | 60.8 | 10 | 0.314 | 39.2 |

a) $\tau_{f1}$, $\tau_{f2}$: lifetime for the long and short fluorescence component. b) $B_1$, $B_2$: preexponential factor. c) $RI_1$, $RI_2$: relative emission intensity (%).

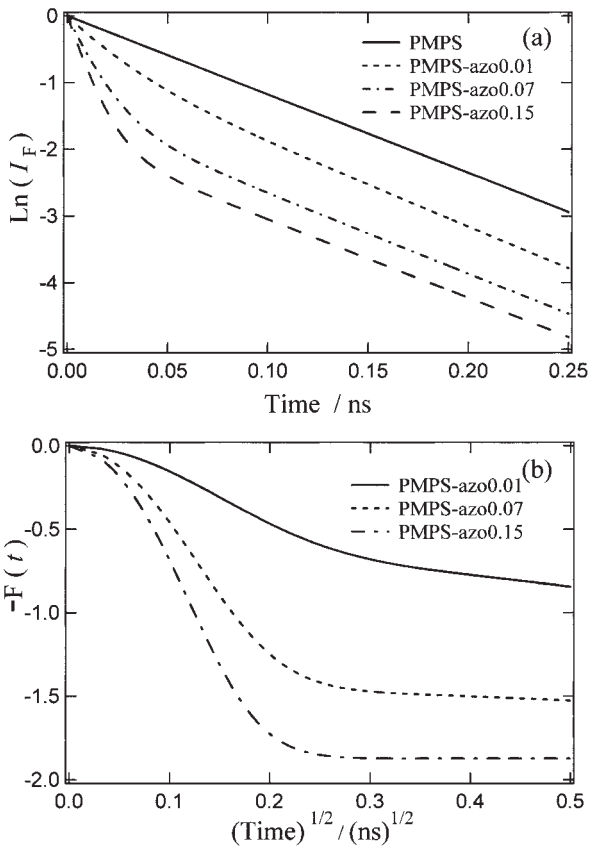


Fig. 8. The fluorescence response functions of PMPS and PMPS-azo (a) and $-F(t)$ versus $t^{1/2}$ for PMPS-azo (b).

ven by the following equation:

$$-\mathrm{F}(t) = \mathrm{Ln}[I_\mathrm{F}(t)] - \mathrm{Ln}[I_\mathrm{F}{}^0(t)] = -1.127\pi^{3/2}C_\mathrm{A}R_0{}^3(1/\tau_\mathrm{fl})^{1/2}t^{1/2} \quad (9)$$

is the deviation from the single exponential decay determined in the absence of a quencher, $[I_\mathrm{F}{}^0(t)]$, due to the energy transfer. Figure 8b shows $-\mathrm{F}(t)$ versus $t^{1/2}$ for PMPS-azo. Because the plot results in curved lines, it is understood that the fluorescence decay does not obey one-step Förster type kinetics.

It is expected that a closer distance between the Si–Si main chain and the pendant *p*-nitroazobenzene group induces efficient singlet energy transfer, so that the model ignoring such proximity effects may show poor agreement with the experimental data. Other effects, such as intramolecular electron transfer and random distribution of the pendant *p*-nitroazobenzene group, may be responsible for the deviations between experimental and calculated results.

Wallraff et al. suggested that the fluorescence quenching of PMPS by several small electron-deficient molecules was attributed to intermolecular electron transfer.[36] In their report, the value of the free energy change of the photochemical electron transfer reaction ($\Delta G$) was calculated by the Weller equation[41] using the oxidation and reduction potentials of the donor [poly(methylphenylsilane)] and the acceptor (4-hydroxy-4′-nitroazobenzene):

$$\Delta G\ (\mathrm{kcal/mol}) = 23.06[E_{1/2}(\mathrm{ox}) - E_{1/2}(\mathrm{red}) - e_0{}^2/\varepsilon d - E_{0,0}] \quad (10)$$

The oxidation potential $[E_{1/2}(\mathrm{ox})]$ of poly(methylphenylsilane) was reported to be 1.0 V (SCE) in film[42] and the reduction potential $[E_{1/2}(\mathrm{red})]$ of 4-hydroxy-4′-nitroazobenzene was −0.65 V (SCE).[43] If the coulombic energy term ($e_0{}^2/\varepsilon d$) is neglected, the $\Delta G$ value of −46 kcal/mol can be roughly calculated and the electron transfer is expected to be strongly exothermic. However, precise estimation of $\Delta G$ is difficult for the PMPS-azo system at the present stage, because precise values of the oxidation potential and the coulombic energy are not available for this system.

The radical anions of the pendant *trans*-*p*-nitroazobenzene group (545 nm and 580 nm)[44] and the radical cations of PMPS,[45,46] however, were not observed in transient absorption on the nanosecond time scale in our study. It is possible that the rate of forward and back electron transfer may be completed within a picosecond time scale at room temperature.

**The Steady-state Photolysis at Low Temperature.** Figure 9 illustrates the absorption spectral change (a) and the differential absorption spectra (b) of PMPS-azo0.32 before and after irradiation with 266 nm light in MTHF at 77 K. Before irradiation, there are two absorption bands peaked at ca. 340 and 385 nm, which are attributed to the Si–Si main chain and the pendant *trans*-*p*-nitroazobenzene group, respectively. After UV-light irradiation, two new broad absorption bands appeared around 545 and 580 nm. The absorbance of these new bands increases with an increase of the irradiation time. When the sample was warmed up to room temperature, these new bands disappeared. Therefore, the absorption bands are

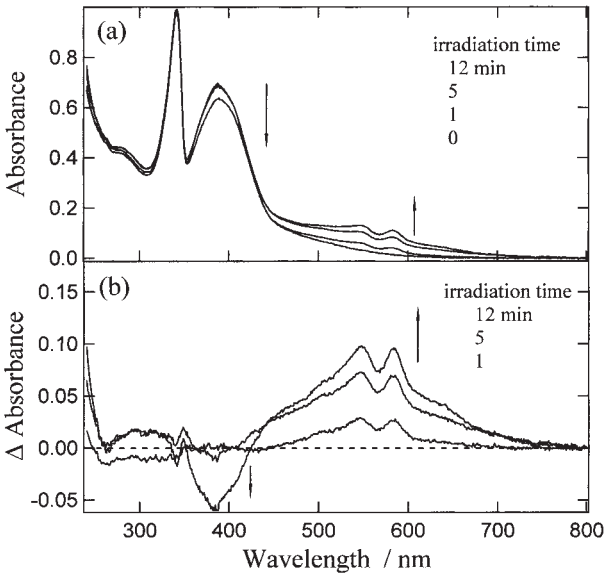


Fig. 9. The absorption spectral change of PMPS-azo0.32 upon irradiation with 266 nm light in MTHF at 77 K (a), and the differential absorption spectra before and after irradiation (b).

ascribable to the photochemical reaction intermediate of PMPS-azo. In a previous paper, we studied the steady-state photolysis and $\gamma$-radiolysis of MNAB in MTHF at 77 K and found that the radical anion produced shows two absorption bands around 545 and 580 nm.[44] According to this result, the photochemical reaction intermediate with absorption maxima at 545 and 580 nm can be assigned to the radical anion of the pendant *trans*-*p*-nitroazobenzene group.

Two processes are considered to be responsible for the formation of the radical anion of the pendant *trans*-*p*-nitroazobenzene group in PMPS-azo. The first is the electron transfer from the Si–Si main chain to the pendant *p*-nitroazobenzene group, because polysilanes are known to be good electron-donors.[47,48] The second process is direct excitation of the pendant *p*-nitroazobenzene group.[44]

In order to confirm the intramolecular electron transfer, quantitative analysis were carried out by the steady-state photolysis of PMPS-azo0.32 and MNAB in MTHF at 77 K, by setting their absorbance for 0.5 at the excitation wavelength (266 nm), as shown in Fig. 10a. The number of photons absorbed by the pendant *p*-nitroazobenzene group was estimated to be ca. 50% of the total number of photons absorbed by PMPS-azo0.32 (Fig. 10a). Figure 10b shows the absorption spectra of PMPS-azo0.32 and MNAB at the irradiation time of 12 min with 266 nm light in MTHF at 77 K. Figure 10c shows the differential absorbance at 545 nm versus the irradiation time. The absorbance of the radical anion formed from PMPS-azo0.32 is always greater than that from MNAB. If only the pendant *p*-nitroazobenzene group is directly excited, the absorbance of the radical anion formed from PMPS-azo0.32 should be half that from MNAB. However, this is not the case. As a result, for the steady-state photolysis of PMPS-azo0.32 in MTHF at 77 K, the intramolecular electron transfer from the Si–Si main chain to the pendant *trans*-*p*-nitroazobenzene group can be pointed out to be responsible for

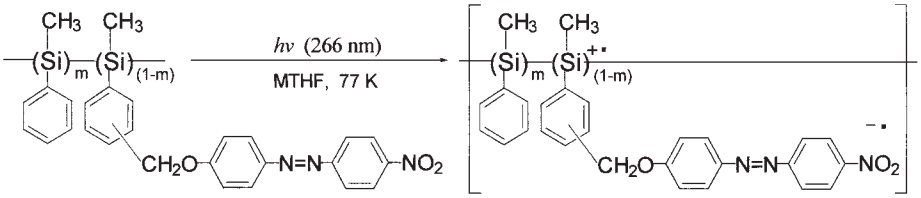


Scheme 2. The intramolecular electron transfer of PMPS-azo in MTHF at 77 K upon the steady-state photolysis.

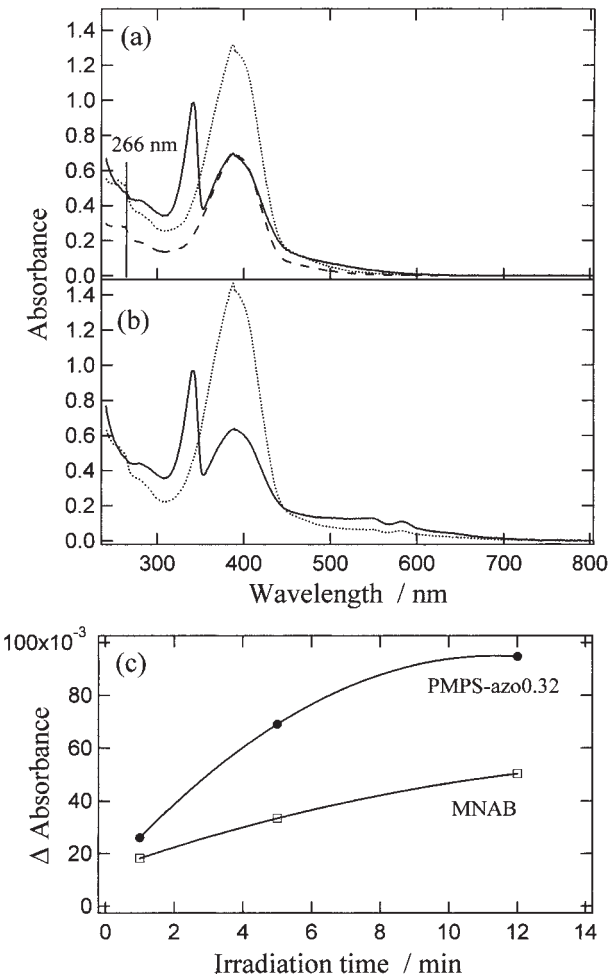


Fig. 10. The absorption spectra of PMPS-azo0.32 (full line) and MNAB (dotted line) in MTHF at 77 K before irradiation, and the normalized absorption spectrum of MNAB (broken line) (a); the absorption spectra of PMPS-azo0.32 (full line) and MNAB (dotted line) after irradiation with 266 nm light at 12 min (b); and the differential absorbance at 545 nm versus the irradiation time (c). The absorbance at irradiation wavelength (266 nm) of two samples was set for 0.5 before irradiation.

the formation of the radical anion, as illustrated in Scheme 2.

The photochemical processes of PMPS-azo0.32 in MTHF at 77 K is described as follows: First, the Si–Si main chain is excited, and then decays radiatively (fluorescence) or non-radiatively via energy transfer and electron transfer. The latter gives rise to the radical anion of the pendant *trans*-*p*-nitroazobenzene group. At the present stage, however, it is difficult to determine the ratio in yield of energy transfer to electron transfer from the Si–Si main chain to the pendant *p*-nitroazobenzene group.

## Conclusions

PMPS-azo with various amounts of the pendant *p*-nitroazobenzene group were synthesized by chloromethylation of PMPS, followed by condensation with potassium salt of 4-hydroxy-4′-nitroazobenzene. The characterization was made by using FT-IR, $^1$H NMR, and GPC spectra.

By the steady-state absorption, fluorescence spectra, and fluorescence lifetime, it was determined that each segment of PMPS-azo consisted of about 16 Si atoms. The fluorescence quantum yields of PMPS-azo decreased with an increase of the mole fraction of the pendant *p*-nitroazobenzene groups. The formation of the radical anion of *trans*-*p*-nitroazobenzene upon the steady-state photolysis of PMPS-azo in MTHF at 77 K indicates that the intramolecular electron transfer takes place. The fluorescence quenching is attributed to the electron transfer and the energy transfer from the Si–Si main chain to the pendant *p*-nitroazobenzene group.

The authors would like to thank Professor T. Nakayama of Kyoto Institute of Technology for his helpful discussion. One of the authors, C. Zhao, thanks the Ministry of Education, Science, Sports and Culture for scholarship support. This work was partly supported by a Grant-in-Aid for Scientific Research from the Ministry of Education, Science, Sports and Culture.

## References

1 R. D. Miller and J. Michl, *Chem. Rev.*, **89**, 1359 (1989).

2 C. L. Callender, C. A. Carere, J. Albert, L. Zhou, and D. J. Worsfold, *J. Opt. Soc. Am. B*, **9**, 518 (1992).

3 F. Kajzar, J. Messier, and C. Rosilio, *J. Appl. Phys.*, **60**, 3040 (1986).

4 H. Yoshida and S. Hayase, *Jpn. Kokai Tokkyo Koho*, JP 11072808 (1999); *Chem. Abstr.*, **130**, 259368 (1999).

5 S. M. Silence, J. C. Scott, F. Hache, E. J. Ginsburg, P. K. Jenkner, R. D. Miller, R. J. Twieg, and W. E. Moerner, *J. Opt. Soc. Am. B*, **10**, 2306 (1993).

6 E. Hendrickx, D. V. Steenwinckel, and A. Persoons, *Macromolecules*, **32**, 2232 (1999).

7 C. Zhan, H. Zeng, J. Qin, D. Liu, N. Cheng, and Y. Cui, *Synthetic Metals*, **84**, 397 (1997).

8 H. Tang, J. Luo, J. Qin, H. Kang, and C. Ye, *Macromol. Rapid Commun.*, **21**, 1125 (2000).

9 F. C. Schilling, A. J. Lovinger, J. M. Zeigler, D. D. Davis, and F. A. Bovey, *Macromolecules*, **22**, 3055 (1989).

10 X. Zhang and R. West, *J. Polym. Sci., Polym. Chem. Ed.*, **22**, 159 (1984).

11 R. West, *J. Organomet. Chem.*, **300**, 327 (1986).

12 T. J. Cleij, J. K. King, and L. W. Jenneskens, *Macromolecules*, **33**, 89 (2000).
13 L. A. Harrah and J. M. Zeigler, *Macromolecules*, **20**, 601 (1987).
14 Y. R. Kim, M. Lee, J. R. G. Thorne, R. M. Hochstrasser, and J. M. Zeigler, *Chem. Phys. Lett.*, **145**, 75 (1988).
15 T. Seki, N. Tainigaki, K. Yase, A. Kaito, T. Tamaki, K. Ueno, and Y. Tanaka, *Macromolecules*, **28**, 5609 (1995).
16 D. Terunuma, K. Nagumo, N. Kamata, K. Matsuoka, and H. Kuzuhara, *Chem. Lett.*, **1998**, 681.
17 Y. Nakano, S. Murai, R. Kani, and S. Hayase, *J. Polym. Sci., Part A: Polym. Chem.*, **31**, 3361 (1993).
18 I. Kminek, E. Brynda, and W. Schnabei, *Eur. Polym. J.*, **27**, 1073 (1991).
19 S. Nešpůrek, F. Schauer, and A. Kadashchuk, *Monatsh. Chem.*, **132**, 159 (2001).
20 H. Tachibana, H. Kishida, and Y. Tokura, *Appl. Phys. Lett.*, **77**, 2443 (2000).
21 W. E. Moerner and S. M. Silence, *Chem. Rev.*, **94**, 127 (1994).
22 L. Yu, W. Chan, and Z. Bao, *Macromolecules*, **26**, 2216 (1993).
23 R. G. Kepler, J. M. Zeigler, L. A. Harrah, and S. R. Kurtz, *Phys. Rev. B*, **35**, 2818 (1987).
24 S. Mimura, T. Nakamura, H. Naito, T. Dohmaru, and S. Satoh, *J. Non-Cryst. Solids*, **227-230**, 543 (1998).
25 G. C. Dismukes and J. E. Willard, *J. Phys. Chem.*, **80**, 2072 (1976).
26 I. A. Mcculloch and R. T. Bailey, *Mol. Cryst. Liq. Cryst.*, **200**, 157 (1991).
27 D. Schulte-Frohlinde, *Liebigs Ann. Chem.*, **612**, 138 (1958).
28 H. Ban, K. Sukegawa, and S. Tagawa, *Macromolecules*, **20**, 1775 (1987).
29 S. J. Holder, A. C. Swain, R. G. Jones, M. J. Went, and R. E. Benfield, *J. Polym. Prep.*, **36**, 312 (1995).
30 S. J. Holder, R. G. Jones, and J. J. Murphy, *J. Mater. Chem.*, **7**, 1701 (1997).
31 R. G. Jones, R. E. Benfield, A. C. Swain, S. J. Webb, and M. J. Went, *Polymer*, **36**, 393 (1995).
32 G. Vanermen, C. Samyn, G. S'heeren, and A. Persoons, *Makromol. Chem.*, **193**, 3057 (1992).
33 C. T. Imrie, F. E. Karasz, and G. S. Attard, *Macromolecules*, **26**, 545 (1993).
34 I. B. Berlman, ''Handbook of Fluorescence Spectra of Aromatic molecules,'' Academic Press, New York and London (1965), p. 114.
35 M. Yokoyama, T. Koura, Y. Hiroshige, and S. Notsu, *Chem. Lett.*, **1991**, 1563.
36 G. M. Wallraff, M. Baier, A. Diaz, and R. D. Miller, *J. Inorg. Organomet. Polym.*, **2**, 87 (1992).
37 T. Fujino, S. Y. Arzhantsev, and T. Tahara, *J. Phys. Chem. A*, **105**, 8123 (2001).
38 D. A. Holden, X. X. Ren, and J. E. Guillet, *Macromolecules*, **17**, 1500 (1984).
39 N. J. Turro, ''Modern Molecular Photochemistry,'' University Science Books, Sausalito, California (1978), p. 303.
40 D. Rehm and K. B. Eisenthal, *Chem. Phys. Lett.*, **9**, 387 (1971).
41 G. J. Kavarons and N. J. Turro, *Chem. Rev.*, **86**, 401 (1986).
42 A. F. Diaz and R. D. Miller, *J. Electrochem. Soc.*, **132**, 834 (1985).
43 J. Barek, A. Berka, and V. Borek, *Microchem. J.*, **26**, 221 (1981).
44 C. Zhao, H. Horiuchi, T. Hoshi, M. Hasegawa, M. Kobayashi, and H. Hiratsuka, *Chem. Lett.*, **32**, 124 (2003).
45 A. Watanabe and O. Ito, *J. Phys. Chem.*, **98**, 7736 (1994).
46 S. Irie and M. Irie, *Macromolecules*, **25**, 1766 (1992).
47 M. Kako and Y. Nakadaira, *Bull. Chem. Soc. Jpn.*, **73**, 2403 (2000).
48 H. Watanabe, T. Muraoka, M. Kageyama, K. Yoshizumi, and Y. Nagai, *Organometallics*, **3**, 141 (1984).